Coaxial electrospinning of microfibres with liquid crystal in the core

Jan P. F. Lagerwall,*[a] Jesse T. McCann,[b] Eric Formo,[b] Giusy Scalia*[cd] and Younan Xia*[b]

Liquid crystal containing composite fibres were produced via coaxial electrospinning, demonstrating that this technique can be used for producing new functional fibres and/or to study the impact of extreme confinement on liquid crystal phases.

Electrospinning offers a simple yet versatile means of producing nano- and microfibres of various materials and with properties tailored for use in diverse applications, ranging from photovoltaics[1] and photocatalysis[2] to energy storage[3] or tissue engineering.[4] By applying a DC voltage of several kV between a spinneret and a collector, a thin jet is ejected from a polymer melt or solution that is pumped through the spinneret. The jet is further stretched and thinned on the way to the collector due to electrostatic self repulsion. During the past few years a number of important advances in the technique were reported, such as fibre alignment,[5,6] tuning of fibre diameter from the nanometre to the micrometre range,[6] combination with sol–gel processes for the production of inorganic tubes,[7,8] and coaxial electrospinning of different polymers[9] or even of non-polymeric liquids in a polymer–inorganic composite sheath.[3,8] While the latter has so far been demonstrated using simple alkanes[3] or mineral oil,[8] such coaxial electrospinning opens the door to incorporation of a wide range of materials, including complex fluids, allowing for the introduction of new functionality to the fibre. As an example of such development we here report coaxial electrospinning of composite fibres consisting of a poly(vinylpyrrolidone) (PVP)/TiO_2 sheath and a nematic liquid crystal core.

Liquid crystals constitute a unique class of liquids in that they combine fluidity with long-range order, orientational and in some cases also 1D or 2D translational.[10] This gives them a strong response to external influences, which is the basis for their very successful application in devices such as displays, modulators and sensors. The nematic phase exhibits only orientational order, described by the director n, a signless unit vector indicating the average direction of the principal symmetry axis of the molecules or molecule aggregates (rod- or disclike). When incorporated into an electrospun fibre, the various types of self-assembled nano- and microstructures and the strong response function could provide the fibre with novel functionality, with potential application fields ranging from cheap temperature sensors to clothing with switchable textures. On the other hand, electrospinning such a composite fibre also constitutes a simple method of studying the effects of extreme confinement on various liquid crystal phases and phase transitions. Such effects can be very strong.[11,12]

Our coaxial electrospinning set-up is schematically shown in Fig. 1. A small hole was made in the side of a syringe containing the outer fluid, allowing a flexible polyimide-coated silica capillary tube (outer diameter 320 μm) to be inserted and led through the needle of the syringe (inner diameter 500 μm). The hole was sealed with epoxy, fixing the capillary tube in position, and the end of the tube was cut parallel with the needle end. The other end of the capillary was attached to the needle of a second syringe, containing the liquid crystalline inner fluid, and each syringe was placed in a separate pump for individual flow control of the two liquids. The high voltage power supply was connected with one lead to the needle of the syringe containing the outer fluid, the other to the target electrode.

We spun fibres containing a room temperature nematic liquid crystal (melting point <0 °C, clearing point 80 °C), the commercial multicomponent mixture Roche RO-TN-403/015S. Although it contains a small amount of chiral dopant, the pitch of the resulting helical modulation[10] is so long that the mixture in this study for all practical purposes can be regarded as an achiral nematic. The outer fluid was a solution of PVP in ethanol, with
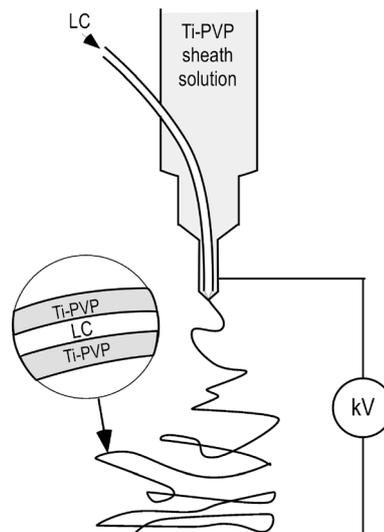
[a] Martin Luther University Halle-Wittenberg, Institute of Chemistry, Muehlpforte 1, 06108 Halle, Germany.
  E-mail: jan.lagerwall@lcsoftmatter.com; Fax: +49 345 5527 400; Tel: +49 345 5525 836
[b] Department of Biomedical Engineering, Washington University, Saint Louis, Missouri 63130, USA.
  E-mail: xia@biomed.wustl.edu
[c] Max Planck Institute for Solid State Research, Heisenbergstr. 1, 70569 Stuttgart, Germany
[d] ENEA CR Portici, 80055 Portici, NA, Italy.
  E-mail: giusy.scalia@solcanta.com

Fig. 1 Schematic drawing (not to scale) of the coaxial electrospinning set-up and the resulting liquid crystal containing composite fibre.

titanium isopropoxide and acetic acid added as sol–gel precursor and catalyst, respectively. Gelation occurs during spinning as the ethanol evaporates and atmospheric water hydrolyses the titanium isopropoxide. The feed rates were in the ranges 0.4–1 mL h^{-1} and 0.2–0.5 mL h^{-1} for the sheath solution and liquid crystal, respectively. The spinneret–collector distance was about 5 cm, and the spinning voltage was varied between 10 and 15 kV. Both liquid reservoirs were kept at room temperature.

The obtained fibres were characterized by scanning electron microscopy (SEM), optical microscopy and Raman spectroscopy. Fig. 2 shows SEM images of a non-woven (a) and an aligned sample (b) and a differential interference contrast optical microscopy image of a sparsely covered sample (c). With our choice of spinning parameters we obtained relatively thick fibres, ranging from some hundreds of nanometres to about a micrometre in diameter. The correlation between flow rates for inner and outer fluids was very important, as non-optimal settings led to beaded fibres, such as the mainly horizontal fibre in (c). Likewise, the degree of filling by liquid crystal depended strongly on the spinning conditions as detected by optical microscopy and Raman spectroscopy, some fibres showing no trace of liquid crystal cores whereas this was clearly present in others. By fine-tuning all spinning parameters bead-free fibres with a high degree of liquid crystal filling could be obtained. The morphology is typical of electrospun fibres with this sheath material,[3,8,13] hence the liquid crystal core has not influenced the morphology, as expected for a simple nematic. A stronger influence might result when spinning a

fibre containing more complex liquid crystal phases, with a higher degree of order, e.g. chiral nematics, columnar phases or smectics. Such experiments are soon to be carried out in our laboratory.

In order to verify that the liquid crystal was indeed incorporated into the fibres and to investigate its alignment we employed polarized Raman spectroscopy, cf. Fig. 3. The measurements were carried out on a single fibre (outer diameter slightly below 1 µm) in which the liquid crystal had been incorporated during spinning, using a Jobin-Yvon Labram Micro-Raman set-up at 633 nm excitation wavelength with high magnification (laser spot diameter ~ 2 µm) and with a polarization scrambler before the detector to rule out instrument artifacts. Accurate sample temperature control was achieved using a Linkam hot stage. Reference spectra of the nematic mixture on its own, in a bulk sample, as well as that of an unfilled TiO$_2$–PVP fibre sample were also obtained, as shown in the bottom section of the diagram in Fig. 3. Within the energy window investigated and at the selected excitation wavelength, the unfilled fibre has only one peak overlapping with a liquid crystal peak, and its response is much weaker than that of the liquid crystal (the plots in Fig. 3 do not share the same scaling), making the Raman characterization with respect to liquid crystal content in the fibres straight-forward.

Raman spectra of the liquid crystal containing fibre are shown in the upper section of Fig. 3, for polarization parallel and perpendicular to the fibre direction, respectively, and at three selected temperatures. The presence of the same peaks in these spectra as in the bulk nematic reference spectrum clearly
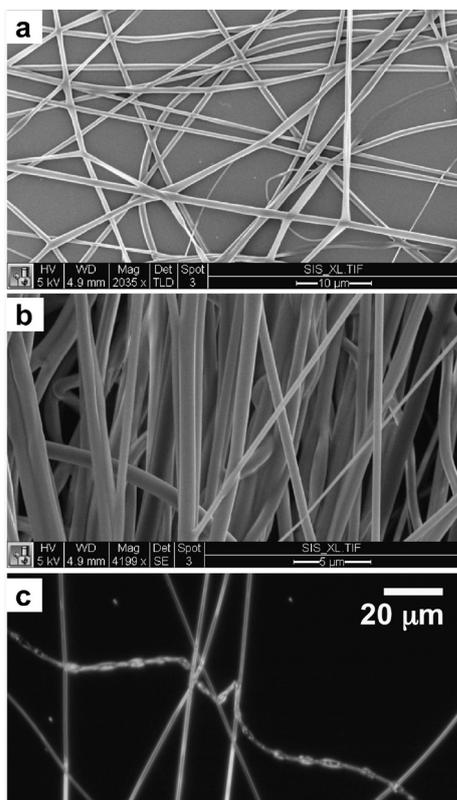

Fig. 2 Fibres consisting of liquid crystal core and TiO$_2$–PVP sheath, which were observed by SEM (a; non-woven, b; aligned sample) and by differential interference optical microscopy (c). The fibres were spun with a sheath solution feed rate of 0.4 mL h^{-1} and a liquid crystal feed rate of 0.2 (a, b) or 0.3 (c) mL h^{-1}.
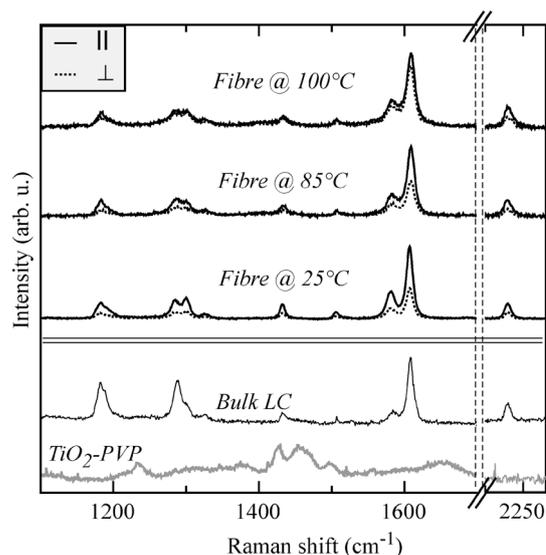

Fig. 3 Raman spectra of an electrospun TiO$_2$–PVP fibre containing the liquid crystal mixture in the core, at three different temperatures surrounding the clearing point of the bulk liquid crystal (top section). The solid-line and dotted-line spectra were obtained with polarization along and perpendicular to the fibre, respectively. In the bottom section, reference spectra of a bulk sample of the liquid crystal at room temperature (black curve) and of a non-filled TiO$_2$-PVP composite fibre (grey curve) are shown. For clarity, the different sets of spectra have been normalized and offset vertically with respect to each other, and the pure TiO$_2$–PVP composite spectrum has been greatly magnified compared to all other spectra, since otherwise none of its peaks would be visible.

shows that the liquid crystal mixture is present in the fibre, and the difference in intensity of the room temperature peaks obtained with different polarizations shows that the nematic phase is aligned with *n* preferentially along the fibre direction: the intensity of the Raman response depends sensitively on the director orientation with respect to the excitation polarization, in a way that can be quite complex,[14] but for the peaks considered here their intensity is maximum when the polarization is parallel to *n*. Spectra were also obtained from beaded fibres like the mainly horizontal one in Fig. 2c. While the liquid crystal spectrum was very strong in the beads, there was no polarization sensitivity, demonstrating that *n* was not aligned. A non-beaded fibre morphology is thus a prerequisite for reliable liquid crystal orientation.

The 85 °C spectra in Fig. 3 are very interesting: despite the fact that they were obtained above the clearing temperature of the bulk liquid crystal, the polarization sensitivity of the response is almost as strong as at room temperature, revealing that the mixture inside the fibre is still nematic. The ratio between the intensities for polarization parallel and perpendicular to the fibre of the most prominent liquid crystal peak (aromatic ring stretching, 1610 cm^{-1}) is plotted as a function of temperature in Fig. 4. The same behaviour was observed for the slightly weaker cyano group stretching mode (2230 cm^{-1}). While the anisotropy decreases monotonously (within experimental error) as expected, the ratio remains above 1 (which would correspond to an isotropic state) throughout the temperature range investigated, a weak anisotropy being detected even at 100 °C. Moreover, the first-order character typical of nematic–isotropic transitions seems to have been lost. The nematic state of the mixture has obviously been stabilized and the transition to the isotropic state smeared out by the confinement in the fibre, in a similar way to what has been observed on nematic liquid crystals filled into nanoporous matrices, see *e.g.* ref. 12. While one cannot rule out that the increase in clearing point to some extent is related to a slight change in composition of the mixture due to a chromatography effect during spinning, such a scenario cannot explain the loss of first-order character, suggesting that confinement is the dominating factor behind the observation. Furthermore, the similarity of bulk and fibre Raman spectra suggests that separation of constitutents—if present—has occurred only to a small degree. On cooling back to room temperature a distinctly anisotropic Raman response was recovered, with stronger response for polarization along the
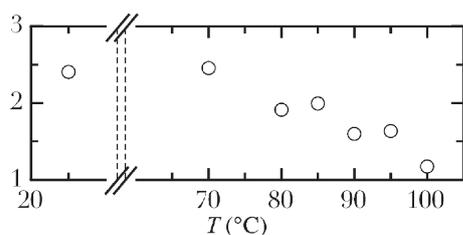
fibre, showing that the nematic phase reformed with the original alignment upon cooling.

In summary we have shown that thin composite fibres with a core of nematic liquid crystal can be produced by coaxial electrospinning. The director was aligned along the fibre and the range of the nematic phase was substantially extended through a confinement-induced up-shift of the clearing temperature by ~20 °C. The method provides an easy way to study confinement effects on liquid crystals by incorporating selected mesomorphic materials and systematically varying fibre diameter and/or core–sheath ratio. By incorporating more complex phases, *e.g.* chiral nematic (cholesteric), columnar or smectic phases (which can be ferro- and antiferroelectric), the technique should allow new functionality to be added to the fibres. Also water-based lyotropic liquid crystals, including phospholipid bilayer phases, may be interesting to spin, although this will require a different sheath solution in order to ensure immiscibility of the two spinning solutions.[8]

Notes and references

1 K. Onozuka, B. Ding, Y. Tsuge, T. Naka, M. Yamazaki, S. Sugi, S. Ohno, M. Yoshikawa and S. Shiratori, *Nanotechnology*, 2006, **17**, 1026–1031.
2 M. Jin, X. Zhang, A. V. Emeline, Z. Liu, D. A. Tryk, T. Murakami and A. Fujishima, *Chem. Commun.*, 2006, 4483–4485.
3 J. McCann, M. Marquez and Y. Xia, *Nano Lett.*, 2006, **6**, 2868–2872.
4 P. D. Dalton, K. Klinkhammer, J. Salber, D. Klee and M. Moller, *Biomacromolecules*, 2006, **7**, 686–690.
5 A. Bianco, G. Iardino, A. Manuelli, C. Bertarelli and G. Zerbi, *ChemPhysChem*, 2007, **8**, 510–514; M. V. Kakade, S. Givens, K. Gardner, K. H. Lee, D. B. Chase and J. F. Rabolt, *J. Am. Chem. Soc.*, 2007, **129**, 2777–2782; Y. F. Yao, Z. Z. Gu, J. Z. Zhang, C. Pan, Y. Y. Zhang and H. M. Wei, *Adv. Mater.*, 2007, **19**, 3707; R. Dersch, T. Liu, A. Schaper, A. Greiner and J. Wendorff, *J. Polym. Sci., Part A*, 2003, **41**, 545–553.
6 D. Li and Y. Xia, *Adv. Mater.*, 2004, **16**, 1151–1170.
7 S. H. Zhan, D. R. Chen, X. L. Jiao and Y. Song, *Chem. Commun.*, 2007, 2043–2045.
8 D. Li and Y. Xia, *Nano Lett.*, 2004, **4**, 933–938.
9 M. L. Ma, V. Krikorian, J. H. Yu, E. L. Thomas and G. C. Rutledge, *Nano Lett.*, 2006, **6**, 2969–2972; Y. Zhang, Z. Huang, X. Xu, C. Lim and S. Ramakrishna, *Chem. Mater.*, 2004, **16**, 3406–3409; D. Li, A. Babel, S. Jenekhe and Y. Xia, *Adv. Mater.*, 2004, **16**, 2062; Z. Sun, E. Zussman, A. Yarin, J. Wendorff and A. Greiner, *Adv. Mater.*, 2003, **15**, 1929.
10 *Handbook of liquid crystals*, ed. D. Demus, J. W. Goodby, G. Gray, H.-W. Spiess and V. Vill, Wiley-VCH, Weinheim, 1998.
11 M. Steinhart, S. Zimmermann, P. Goring, A. K. Schaper, U. Gosele, C. Weder and J. H. Wendorff, *Nano Lett.*, 2005, **5**, 429–434; T. Jin, B. Zalar, A. Lebar, M. Vilfan, S. Zumer and D. Finotello, *Eur. Phys. J. E*, 2005, **16**, 159–165; R. L. Leheny, S. Park, R. J. Birgeneau, J. L. Gallani, C. W. Garland and G. S. Iannacchione, *Phys. Rev. E*, 2003, **67**, 011708; J. P. F. Lagerwall, D. D. Parghi, D. Krüerke, F. Gouda and P. Jägemalm, *Liq. Cryst.*, 2002, **29**, 163–178.
12 G. S. Iannacchione, G. P. Crawford, S. Qian, J. W. Doane and D. Finotello, *Phys. Rev. E*, 1996, **53**, 2402–2411.
13 J. McCann, D. Li and Y. Xia, *J. Mater. Chem.*, 2005, **15**, 735–738.
14 S. Jen, N. A. Clark, P. Pershan and E. Priestley, *J. Chem. Phys.*, 1977, **66**, 4635–4661.

Fig. 4 Ratio of the intensities for polarization parallel and perpendicular to the fibre, respectively, of the aromatic ring stretching Raman mode, as a function of temperature.